Temperature dependence of de Gennes narrowing and transport properties of liquid rubidium: Experimental and simulation results

D. Bertolini*
Istituto per i Processi Chimico-Fisici del Consiglio Nazionale delle Ricerche, Via Moruzzi 1, I-56124 Pisa, Italy

F. Demmel
ISIS Facility, Rutherford Appleton Laboratory, Chilton OX11 0QX, United Kingdom

A. Tani
Dipartimento di Chimica e Chimica Industriale, Universita' di Pisa, Via Risorgimento 35, I-56126 Pisa, Italy
(Received 22 May 2007; published 27 September 2007)

Recent neutron scattering results [F. Demmel *et al.*, Phys. Rev. B **73**, 104207 (2006)] on the temperature dependence of de Gennes narrowing in liquid rubidium have stimulated a molecular dynamics (MD) study in the same temperature and density range. At the k value of the first peak of $S(k)$, the MD results agree very well with experimental data of $\tilde{S}(k_{\max},\omega=0)$, $F(k_{\max},t=0)$, and longitudinal viscosity $\eta_L(k_{\max},\omega=0)$. Other transport properties, such as self-diffusion and shear viscosity, are also accurately reproduced. At $k=0$, on the other hand, the MD results significantly underestimate the experimental values of bulk viscosity and thermal conductivity. For the latter, this is a well known deficiency of models which do not explicitly take into account the electronic contribution to thermal exchanges. However, the large difference between MD and macroscopic experimental data for bulk viscosity casts some doubts on its indirect calculation from sound absorption data. This contradictory result, which presumably extends to all alkali metals, is discussed in the light of various theoretical models.

DOI: 10.1103/PhysRevB.76.094204 PACS number(s): 61.20.−p, 61.25.−f, 66.20.+d, 78.70.Nx

I. INTRODUCTION

In the last 30 years, many theoretical,[1,2] experimental,[3,4] and computer simulation studies[5–9] have been devoted to the dynamics of liquid metals. In particular, recently the inelastic x-ray scattering of synchrotron radiation[10] has been introduced and the first-principles and *ab initio* computational approach[7,8] has been applied in the simulation of liquid metals, to overcome the limitations of pseudopotentials[5] and embedded models.[6] Moreover, very recently the *ab initio* approach, much more time expensive than the standard simulation methods, has been used for liquid rubidium near the critical density,[11] to study the variation of atomic and electronic structures in a wide region of the coexistence curve and to identify the presence of clusters (especially dimers) and bound states. *Ab initio* simulations have recently also been used in the study of transport properties of some liquid metals.[9,12] Even if the physical time span and the number of atoms are significantly smaller than for typical classical simulations, these papers prove that this kind of calculation is feasible for liquid metals. On the other hand, from the experimental point of view, the tendency is to extend the temperature range of the data for the phonon dispersion curves, the diffusion processes, and the k-ω dependence of the transport coefficients. Along this line, Demmel *et al.*[13] have measured the coherent structure factor $\tilde{S}(k,\omega)$ in a wide range of temperature with neutron scattering (NS) techniques at $k_{\max}$, the k value corresponding to the maximum of $S(k)$ (de Gennes narrowing range). This way, also information on the temperature dependence of the generalized longitudinal viscosity $\eta_L(k_{\max})$ has been obtained. Later on,[14] the same authors extended the measurements to a wide k range ($4\ \mathrm{nm}^{-1} < k < 25\ \mathrm{nm}^{-1}$) observing as the most striking feature a frequency change with rising temperature in the inelastic excitations at a momentum transfer of $\sim 4.5\ \mathrm{nm}^{-1}$, i.e., the minimum k value explored ($\sim 4.5\ \mathrm{nm}^{-1}$).

The main goal of the present work is to employ molecular dynamics (MD) simulation methods to analyze these phenomena in the same temperature range and, in particular, to extend the study of their temperature dependence to other transport properties and the whole k-ω range. In Sec. II we report the simulation details and discuss the features of the potential used. In Sec. III A we compare the NS and MD results for the $k_{\max}$ value. Section III B is devoted to a comparison of the MD self-diffusion results with the corresponding experimental data and to an analysis of the deviation from Fick's law for this potential. Section III C addresses thermal conductivity, whose deviation from experimental data can be readily traced back to the missing electronic contributions entailed by the model interactions adopted. On the other hand, a more extensive discussion of the behavior of shear, bulk, and longitudinal viscosities is necessary (Sec. III D). This seems to indicate that, in the case of bulk viscosity, the experimental values might significantly be overestimated. Finally, the most important conclusions are collected in Sec. IV.

II. SIMULATION DETAILS

The effective potential adopted for the simulation models the rubidium atoms as an ensemble of metallic ions interacting with each other through screened Coulombic forces. The form proposed by Price *et al.*[15] reads

$$u(r) = \frac{(Ze)^2}{r}\left[1 - \frac{2}{\pi}\int_0^\infty dq G(q)\frac{\sin(qr)}{q}\right],$$

where Ze is the ionic charge and $G(q)$ contains the bare ion pseudopotential form factor and the q dependent dielectric function. This potential is the same as the one employed by Balucani *et al.* to show that equilibrium and time dependent correlation functions become the same for all alkali metals, if a properly scaled form is adopted.[16] A somewhat different parametrization has been used by Wax *et al.* in their study of diffusion as a function of temperature.[17]

Simulation runs have been carried out on systems of 864 particles arranged in a cubic box whose size has been adjusted to the desired density, which was kept fixed. Hence the simulation conditions correspond to that of a microcanonical ensemble. This choice has been made not to affect the particle dynamics through the velocity rescaling required to fix the temperature at a specified value. The cutoff distance is larger than three times that of the first node of the force, while the integral that enters the expression of the potential has been calculated with a Gauss-Legendre quadrature formula. Each run spans a physical time of at least 0.5 ns after equilibration, with a time step of 5 fs. The temperatures explored ranged from around melting (315 K) to 625 K.

III. RESULTS AND DISCUSSION

A. de Gennes narrowing: Neutron scattering and molecular dynamics results

Very recently Demmel *et al.*[13] have investigated in a coherent inelastic neutron scattering experiment the temperature dependence of de Gennes narrowing in liquid rubidium. In particular, the authors found that at the k value of the first peak of the structure factor ($k_{\max}$) the width of the quasielastic line shows a nearly linear temperature dependence with no significant evidence of a changing slope. This result is confirmed by the MD results reported in Fig. 1, which agree very well with the experimental data. In Fig. 1 two types of results are shown: the first is obtained from the effective width at the 1/2 value of $\tilde{S}(k_{\max},\omega=0)$; the second one by fitting the long time tail of $F(k_{\max},t)$ with an exponential, $\exp(-\Gamma t)$. The second method seems to suggest a decrease of the slope $\Gamma(T)$ at low temperature. As a consequence, the temperature dependence of the amplitude $\tilde{S}(k_{\max},\omega=0)$, associated with the decay of density fluctuation on the long time scale, decreases in a nonlinear manner indicating a change in dynamics at about $1.5T_m$ (melting temperature). As Fig. 2 shows, this effect is also present in the MD results. Also the values of $F(k_{\max},t=0)\equiv S(k_{\max})$ agree well with the experimental results (see Fig. 2). However, as far as the width behavior is concerned, the temperature dependence of $S(k_{\max})$ is much more linear compared to $\tilde{S}(k_{\max},\omega=0)$. The difference between MD and experimental data for $\tilde{S}(k_{\max},\omega=0)$ near the melting point could be related to not well resolved deconvoluted experimental data. MD and experimental values of generalized longitudinal viscosity are compared in Fig. 3 for $k_{\max}$. They are obtained from the following relation:

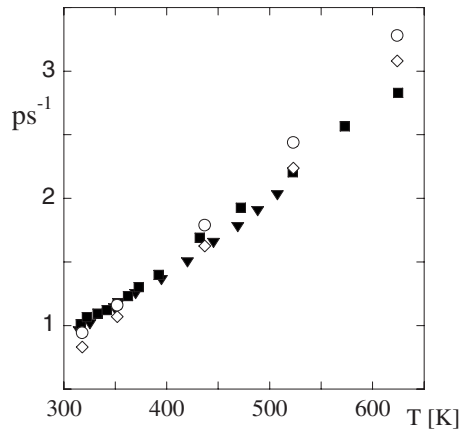

FIG. 1. Full width at half maximum of the experimental and simulation data of $\tilde{S}(k_{\max},\omega)$: the black triangles and squares are the IN3 and FRM results, respectively (Ref. 13); the white rhombi are our MD results, obtained from the abscissa corresponding at 1/2 of $\tilde{S}(k_{\max},\omega=0)$ and the white circles are obtained from an exponential fit of the long time behavior of $F(k_{\max},t)$.

$$\eta_L(k) = \rho\frac{k_BT}{M}\frac{\tilde{S}(k,\omega=0)}{S(k)^2}. \quad (1)$$

In this expression of the generalized longitudinal viscosity the temperature-density contribution is neglected [see, for example, Eqs. (2) and (5) of Ref. 18]. Equation (1) differs for a factor π from Eq. (3) of Ref. 13 due to a different definition of the Laplace transform. The approximation of neglecting the second term of Eq. (5) of Ref. 18 is verified at all simulation temperatures. MD results show a monotonic in-

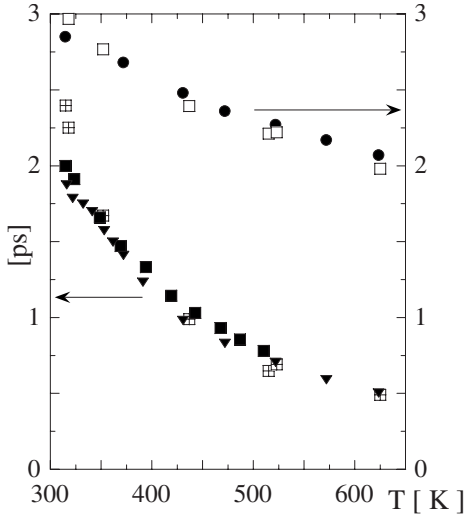

FIG. 2. $\tilde{S}(k_{\max},\omega=0)$ as a function of temperature: the black symbols show experimental results obtained by neutron scattering (Ref. 13); the white crossed squares are our MD results (scale on the left); $S(k_{\max})$ as a function of temperature: the black circles are experimental data from Ref. 13 and the white squares our MD results (scale on the right).

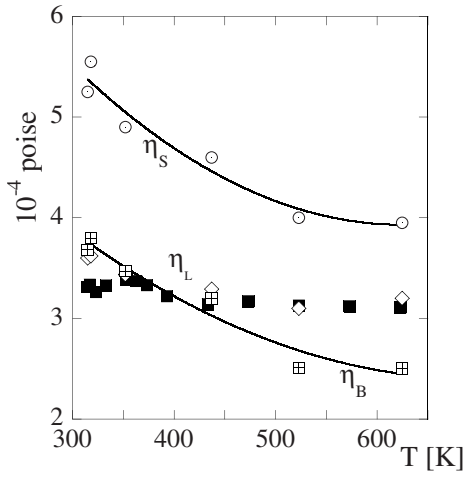

FIG. 3. Generalized viscosities of liquid rubidium at $k=k_{\max} \simeq 15\ \mathrm{nm}^{-1}$: the black squares are experimental results (taken from Ref. 13) and the white rhombi are MD results of longitudinal viscosity, η_L; the white circles are MD results of shear viscosity; η_S; the white crossed squares are MD results of bulk viscosity, η_B; and the continuous lines through η_S and η_B are only a guide to the eyes.

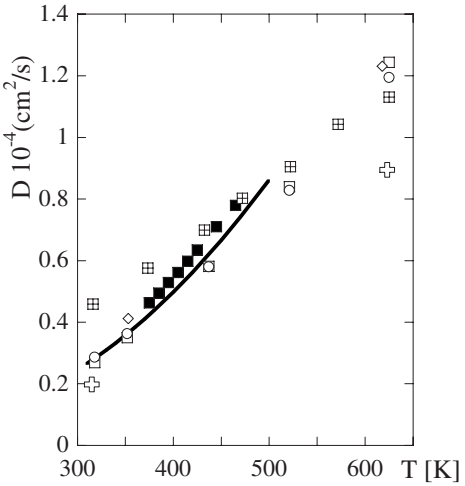

FIG. 4. Self-diffusion coefficients as a function of temperature: the black squares and continuous line are experimental results of Refs. 28 and 29; the white crossed squares show the Enskog self-diffusion of Fig. 5 of Ref. 13 derived from the width of the experimental structure factor; the white squares and white circles our MD results of D_{GK} and D_{r^2}, respectively; the white rhombi MD results of Bretonnet (Ref. 30); the white crosses from the long time behavior of the self-part of the intermediate MD scattering function, $F_S(k_{\max},t)$, see text.

crease when T approaches the melting point while experimental data exhibit a little maximum. The same figure also reports the results of the generalized shear viscosity calculated with the standard relation

$$\eta_S(k) = \rho \frac{k_B T}{M k^2} \frac{1}{\tilde{C}_T(k,\omega=0)}. \tag{2}$$

This definition is the same as that of Eqs. (4) and (8) of Ref. 18 with ρ the liquid density and $\tilde{G}_{22,T}(k,0)=\tilde{C}_T(k,0)/C_T(k,0)$ the spectra of the normalized transverse current, with $C_T(k,t=0)=k_BT/M$.

We refer the reader to Ref. 18 for a discussion of the generalized bulk viscosity behavior. In the same paper [see Eqs. (3), (6), and (7)] details on how to obtain the MD values of $\eta_B(k)$ at finite k are provided. Conversely the $k=0$ data are calculated by Green-Kubo integration of the relevant time correlation functions. We wish to remark that negative values of bulk viscosity would be obtained using the relation $\eta_B(k)=\eta_L(k)-4/3\,\eta_S(k)$ at $k_{\max}$, being $\eta_S(k_{\max})>\eta_L(k_{\max})$ (see Figs. 1 and 2 of Ref. 18). Qualitatively, the results of Fig. 3 are similar to that obtained for argon, also at $k_{\max}$ and close to its melting point, i.e., 88 K (see Fig. 2 of Ref. 18). In fact $\eta_L(k_{\max}) \simeq \eta_B(k_{\max})$ and $\eta_S(k_{\max})$ is larger by $\sim 60\%-70\%$. However, the viscosities increase as temperature decreases much more clearly in rubidium then in argon, where they seem constant or slightly decreasing as temperature decreases (see Fig. 2 of Ref. 18). Probably, the latter effect is related to a different behavior of density: in fact, for argon the density at 88 K ($\rho=1.3\ \mathrm{g/cm^3}$) is lower than at 200 K ($\rho=1.4\ \mathrm{g/cm^3}$), while for liquid rubidium $\rho=1.47\ \mathrm{g/cm^3}$ near melting point, $T=315$ K, but $\rho=1.35\ \mathrm{g/cm^3}$ at higher temperature, $T=624$ K.

Though in the past many papers have dealt with dynamic properties of liquid rubidium and alkali metals, both from the experimental[19–22] and MD simulation points of view,[23–27] still many issues deserve further study. So far, we compared experimental and MD results at $k_{\max}$, i.e., the value where the maximum of $S(k)$ is found. This corresponds to the range of distances where positional correlations among the system particles are strong and slow down the decay of density fluctuations (de Gennes narrowing). In the following, we extend to $k=0$ the comparison with the corresponding experimental results of various dynamic properties for liquid rubidium, with particular emphasis on viscosities.

B. Self-diffusion

Experimental data[28,29] and MD results of self-diffusion coefficients are reported in Fig. 4 as a function of temperature. Our MD results, either obtained from the velocity correlation function via the standard Green-Kubo formula, D_{GK}, or from the mean square displacement, D_{r^2}, agree well with that computed by Bretonnet[30] adopting a slightly different potential.[31] Overall, all sets of MD results satisfactorily reproduce the experimental values and their temperature dependence. Figure 4 also includes derived Enskog self-diffusion D_E coefficients (see Fig. 5 of Ref. 13), calculated from the width of the experimental $\tilde{S}(k,\omega)$ at the structure factor maximum. Kinetic theory showed that the width of the coherent scattering law at the structure factor maximum is related to the self-diffusion coefficient. In the Enskog approximation only uncorrelated binary collisions of hard spheres are treated and collective influences are neglected, which results in too large diffusion constants near the melting point. From the long time behavior of the self-part of the calculated intermediate scattering function, $F_S(k_{\max}t)$ diffu-

sion coefficients have been obtained by the relation (strictly valid in the $k \to 0$ limit)

$$D_F(k_{\max}) = -\frac{\partial \ln[F_S(k,t)]}{k^2 \partial t}. \quad (3)$$

Fick's law is the basis of the above relation and the long time behavior delivers smaller diffusion coefficients compared to macroscopic values. For the self-diffusion we also examined the evolution with increasing wave vector. The normalized k-dependent diffusion coefficient $\Delta(k) = D_F(k)/D$ shows in alkali metals a marked oscillatory behavior around 1. Near the melting point, there is a minimum at $k_{\max} \sim 15$ nm^{-1}, followed by a maximum ($k \sim 35$ nm^{-1}) with a gradual transition to the $1/k$ behavior typical of the free particle regime. This behavior is well reproduced by mode coupling theory (MCT). In fact, at $T=315$ K our result is $\Delta(k_{\max})=0.71$ in very good accord with MCT results, see Fig. 3 of Ref. 32. At $T=624$ K we obtain $\Delta(k_{\max})=0.75$.

C. Thermal conductivity

The coefficient of thermal conductivity, λ, has been calculated according to the Green-Kubo relation, i.e., by time integration of the energy flux correlation function, $F_q(t)$,[33]

$$\lambda = \frac{\rho}{MRT^2} \int_0^\infty F_q(t) dt. \quad (4)$$

The same formula was used to obtain the thermal conductivity of hydrogen bonded liquids such as water and hydrogen fluoride.[34] Our MD results at $T=318$ K and $T=624$ K ($\lambda = 0.12 \pm 0.1$ W/m K and $\lambda = 0.11 \pm 0.1$ W/m K, respectively) underestimate the corresponding experimental values ($\lambda = 34.4$ W/m K and $\lambda = 31.7$ W/m K)[35] by some 2 orders of magnitude. This result, however, is not surprising and simply due to neglecting the electronic conductivity, $\lambda_{\rm el}$, as the adopted simulation potential and technique only account for the lattice thermal conductivity, $\lambda_{\rm lat}$. The latter has been shown[36] to be around 1% of the total thermal conductivity for liquid metals near the melting point. As a consequence, the electronic contribution to the thermal conductivity in this type of liquids is overwhelming and $\lambda_{\rm el}$ calculated by the Wiedemann-Franz law, defined by

$$\lambda_{\rm el} = \frac{L_0 T}{\rho_e}, \quad (5)$$

where $L_0 = 2.445 \times 10^{-8}$ W Ω K^{-2} is the Lorenz number and ρ_e the electric resistivity fits the experimental data well, for λ. In fact, the experimental errors are greater than or of the order of the ion contribution.[37]

In conclusion, to obtain a correct value of thermal conductivity by computer simulation it is necessary to explicitly describe the electronic dynamics. Recent work with *ab initio*[12,38–40] methods indicates that the electronic interactions can be taken into account to obtain the thermal conductivity of liquid metals.

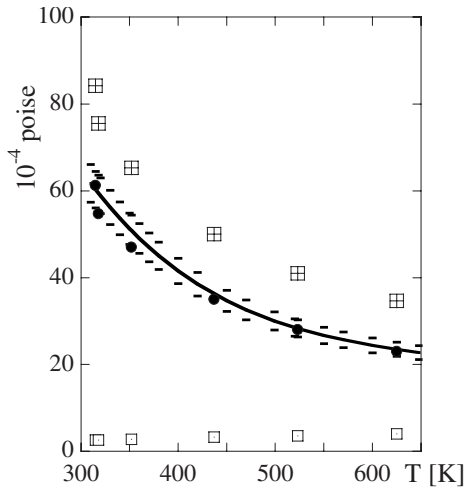

FIG. 5. Temperature dependence of viscosities at $k=0$: continuous curve mean experimental data of shear viscosity, whose uncertainty, roughly ±7%, is also shown around the curve; the white crossed squares, black circles, and white squares are MD results of longitudinal, shear, and bulk viscosities, respectively, computed via Green-Kubo relations, see text.

D. Viscosities

In view of the diverse success of the model potential when modeling diffusion and thermal conductivity, it is of interest to extend the comparison to other transport coefficients, e.g., viscosities. This is depicted in Fig. 5, where we report the MD results of longitudinal, shear, and bulk viscosities as a function of temperature. We recall that also viscosities at $k=0$ are computed by Green-Kubo integration of appropriate time correlation functions. The comparison with the experimental results shows a quite good agreement for η_S (Ref. 41) and its temperature dependence. A much more impressive result is the very low bulk viscosity, η_B, obtained by MD, which remains small throughout the temperature range, despite a slight increase with T, from 2.4×10^{-4} P at $T=315$ K, to 4×10^{-4} P at $T=623$ K. The experimental values reported in Ref. 35 decrease with T, from 250×10^{-4} P at $T=315$ K to 61×10^{-4} P at $T=518$ K so that the ratio η_B/η_S would be 3.73 near the melting point, where the MD result is 0.04. Large values of bulk viscosity are reported by the same authors for the other alkali metals Na, K, and Cs, see Tables I, III, and IV of Ref. 35. Their indirect calculation is based on the relation for ultrasonic absorption as follows:

$$\alpha_{\rm total} = \frac{2\pi^2 f^2}{\rho c_s^3} \left(\frac{4\eta_S}{3} + \frac{(\gamma - 1)\lambda}{C_p} + \eta_B \right), \quad (6)$$

where f is the frequency, c_s is the velocity of sound, $\gamma = C_p/C_v$, and C_p and C_v are the heat capacity at constant pressure and volume, respectively.

The sum of the first two terms is defined as $\alpha_{\rm classical} = \alpha_S + \alpha_T$, while the third term, $\alpha_{\rm excess} = \alpha_{\rm total} - \alpha_{\rm classical} = \alpha_B$, is the bulk viscosity contribution. Kim *et al.*[35] rewrote the second term utilizing the thermodynamic relation

$$(\gamma - 1) = \frac{c_s^2 \beta^2 T}{C_p}, \tag{7}$$

where $\beta = -\partial\rho/\rho\partial T$ is the volume expansion coefficient. Unfortunately, as remarked by the authors, the thermal contribution is dominant and the excess absorption for liquid rubidium with the data used in Ref. 35 is ~14% near the m.p. and ~4% at $T=518$ K. Hence, even a small error in the experimental quantities, especially β and λ, lead to a large error in bulk viscosity, ~60% for liquid rubidium at the m.p., and increasing with temperature. Moreover, the above relation is bound to increasing the error, as the density is accurately known [$\sim(1\pm2)\%$], but β^2 is scattered by as much as 40%–50%. The calculation of $(\gamma-1)$ from the data of Ref. 35 and adopting Eq. (6) delivers 0.091 at $T=316$ K. The values reported in the literature range from 0.097 to 0.150.[3,42,43] 0.097 corresponds to $\eta_B/\eta_S=2.23$ and 0.150 to $\alpha_T > \alpha_{\text{total}}$, as $(\gamma-1)=0.121$ would yield $\eta_B=0$. In any case, the results are much different from $\eta_B/\eta_S=3.73$ of Table III of Ref. 35. Applying Eq. (6) to other alkali metals leads to the same inconsistency. For liquid cesium, e.g., we obtain for $\gamma-1=0.0878$, to be compared with experimental values 0.099, 0.102,[3] and 0.16.[44] For liquid potassium, we obtain 0.105 vs 0.102, 0.105, and 0.11.[3] Finally, for liquid sodium, we obtain 0.096 against 0.091, 0.11, and 0.12.[3] For the latter liquid, more accurate data of λ, β, c_s, and η_S (Ref. 45) and a recalculation of η_B/η_S of Tables I and V of Ref. 35 yield in a value ~20% lower at 373 K and ~33% higher at 516 K. Note that for sodium there is another sound absorption result[46,47] that gives $\eta_B=0$. Conclusive from this survey is that the dominant part in the ultrasound absorption, the thermal contribution, has already a too large spread in experimental values to provide reliable results for the bulk viscosity. Apparently this issue is still unsettled and actually the only experimental route to bulk viscosity is through acoustic absorption measurements, improved by ultrasonic and Brillouin scattering techniques,[48] in all cases resorting to Eq. (6). To our knowledge, the only other experimental method is the shock-wave thickness technique,[49] which, so far, did not provide estimates of η_B.

In the literature we have found only another calculation of viscosities by the Green-Kubo expression and practically the same potential,[15] but with a smaller particle number ($N=108$), to model liquid sodium and potassium.[50] In this case, $\eta_B/\eta_S=0.9$ at 393 K and 1.4 at 573 K for sodium, and 0.18 and 0.125 for potassium, at the same temperatures. These values further decrease at higher temperature. The only other paper we are aware of on liquid metals is on liquid iron[51] at high temperature, approximately that of Earth's outer core (~5000–8000 K, m.p. is $T_m=1808$ K). The authors, using an embedded-atom potential, found that $\eta_B/\eta_S \sim 0.065$ at lower and 0.1 at higher temperature, in complete disagreement with previous estimates.

A possible way to explain the low value of MD bulk viscosity would be to assume that, as in the case of thermal conductivity, the electron and the lattice contribution are of the same order. This hypothesis has been tested from a theoretical point of view in the past by various authors.[52–54] In all papers, adopting an ion-electron plasma approach, the authors have concluded that the electronic contribution to longitudinal viscosity, and hence to bulk viscosity, is completely negligible in liquid metals.

A different approach has been chosen by Zuckerwar and co-worker.[55] Applying a macroscopic phenomenological approach to the translational relaxation in gases, the authors obtain the following relation:

$$\frac{\eta_B}{\eta_S} \simeq \frac{3}{4} \frac{\gamma(\gamma-1)}{C_p} \frac{1}{P_r}, \tag{8}$$

where C_p is the heat capacity, expressed in units of the gas constants, R, and $P_r = \eta_S C_p/M\lambda$ is the Prandtl number, the ratio between the kinematic viscosity and thermal diffusivity. For real liquid metals P_r is very small[56] ($P_r \leqslant 0.01$) and it is 0.01, 0.0075, 0.007, and 0.008 for the alkali metals Na, K, Rb, and Cs, respectively. Taking into account the MD values of η_S and the heat capacity C_p, which are well reproduced in the experimental data, and the simulated thermal conductivity λ, the Prandtl number of rubidium should be ~300 times higher than the experimental value. Thus, for liquid rubidium at m.p. we obtain from Eq. (8) $\eta_B/\eta_S \sim 2$ and $\eta_B/\eta_S \sim 0.007$ using experimental and MD thermal conductivities, respectively. The contrasting result from the two approaches (gaslike and plasmalike) stems from the fact that the bulk viscosity in Eq. (8) is proportional to thermal conductivity, while in plasmalike approaches it is practically independent. This apparent contradiction could be resolved considering that Eq. (8) has been derived neglecting the electron contribution and, as a consequence, this relation can be used for simple nonmetallic liquids. In our case, it would predict results in reasonable accord with the MD results ($\eta_B/\eta_S \ll 1$) and would support the conjecture that the electronic contribution to the bulk viscosity is negligible. Many authors have proposed various approaches to the computation of bulk viscosity in the fluids[57–59] and some of these are discussed in Ref. 55. Some of them[60,61] are based on effective pair distribution $g(r)$ obtained either by computer simulation or from experimental $S(k)$. As the latter is well reproduced by simulation, these methods are bound to yield low value of η_B.

All these considerations seem to support the conclusion that it is not possible to identify the electron contribution to η_B, with these methods.

In principle, a straightforward solution would be to adopt an *ab initio* computer simulation method, thus including the electron contribution to viscosity. Many simulations of this kind can be found in the literature, focusing on the dynamics of alkali metals[62] and, in particular, rubidium.[63] However, no viscosity results are reported. In Ref. 64 shear viscosity data for liquid aluminum, selenium, and Fe-S under Earth's core conditions have been obtained by Green-Kubo first-principles simulation, but again not for longitudinal and bulk viscosities. Some years ago mode coupling theory was applied to describe liquid dynamics of simple classical fluids and, in particular, liquid rubidium.[65] Within this description, neglecting the thermal contribution, an expression for the ratio of the bulk to shear viscosity was derived:

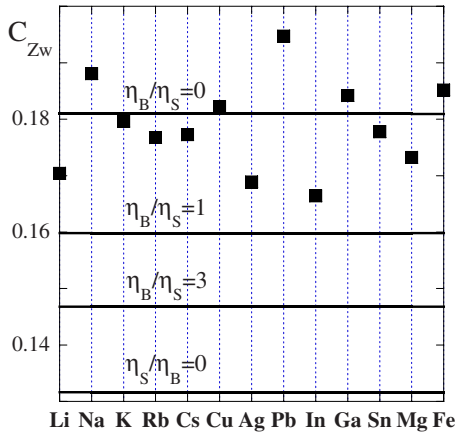

FIG. 6. (Color online) C_{Zw} according to the left side of Eq. (10) by experimental data of transport properties of liquid metals at the melting point, black squares; the horizontal lines correspond to C_{Zw} from the right side of Eq. (10) for $\eta_B/\eta s=0,1,3$ and $\eta_S/\eta_B=0$, respectively.

$$\frac{\eta_B}{\eta_S} = \frac{3}{4}\left(\frac{c_L^2 - c_{\text{th}}^2}{c_T^2}\right)^2 - \frac{4}{3}. \tag{9}$$

Herein are c_L the high frequency sound velocity and c_T the transverse sound velocity, which are both related to the second derivative of the potential. All values are applied in the $k=0$ limit. Inserting $c_L=1570$ m/s, $c_T=842$ m/s,[25] and the isothermal sound velocity $c_{\text{th}}=c_s/\gamma^{1/2}=1260\frac{m}{s}/1.1^{1/2}$ (Refs. 3 and 44) we get a ratio of 0.22, which is more than an order of magnitude smaller than the ultrasound derived ratio. Hence, the extrapolation of MCT also predicts much smaller bulk viscosity values, in agreement with our MD and NS results.

Finally, we would like to discuss a solidlike approach, based on a particular view of the dynamics of cold dense fluids, due to Zwanzig.[66] Applying the normal mode approach to the GK formula for the self-diffusion and introducing the longitudinal and transverse contributions, the author obtains

$$\frac{D\eta_S}{k_BT}\left(\frac{V}{N}\right)^{1/3} = a_Z\left(2 + \frac{\eta_S}{\eta_L}\right) \equiv C_{\text{Zw}}, \tag{10}$$

where the term in parentheses on the left hand side is the volume per particle $v=V/N$, and $a_Z=(3/4\pi)^{1/3}/3\pi=0.065\,82$. Being $\eta_L=\eta_V+4\eta_S/3$, it turns out that $0.1316<C_{\text{Zw}}<0.181$, where the extreme values correspond to $\eta_S/\eta_B=0$ and $\eta_B/\eta_S=0$, respectively. Other authors have analyzed the liquid metals' transport properties with this type of approach,[67,68] but recent papers on the transport coefficients permit a deeper study. Here, the analysis of experimental data of self-diffusion[69–71] and shear viscosity[70–72] in liquid metals is carried out in the light of various models and theory, in particular, the scaling law of Dzugutov[73] and Rosenfeld.[74]

In the following it is convenient to define (as Rosenfeld suggested) the adimensional self-diffusion constant and shear viscosity:

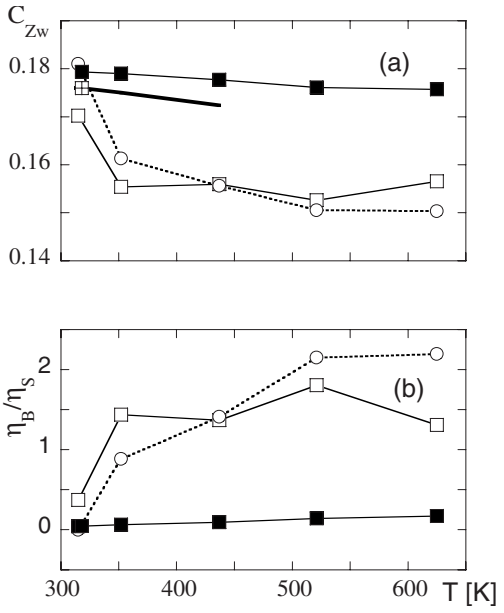

FIG. 7. (a) C_{Zw} of liquid rubidium as a function of temperature: the black squares from MD results of $\eta_L/\eta s$ [see right hand side of Eq. (10)]; the white squares and circles from the left side of Eq. (10) with MD values of D_{GK}, D_{r^2}, and ηs, respectively; the white crossed square at the melting point is from the left side of Eq. (10) with experimental values of D and ηs and the thick continuous line is the temperature dependence corresponding to the same set of data; (b) the black symbols are values of $\eta_B/\eta s$ calculated directly from the MD data; the white symbols are calculated from Eq. (10) by MD values of D_{GK} (squares), D_{r^2} (circles), and ηs.

$$D^{(R)} \equiv D\frac{v^{-1/3}}{(k_BT/M)^{1/2}}, \tag{11}$$

$$\eta_S^{(R)} \equiv \eta_S\frac{v^{2/3}}{(k_BTM)^{1/2}}, \tag{12}$$

where $v^{1/3}$ is a length per particle.

The advantage lies in the fact that the product, $C_{\text{Zw}}=D^{(R)}\eta_S^{(R)}$, is equal to the left side of Eq. (10) and a direct comparison of $D^{(R)}$ and $\eta_S^{(R)}$ is possible for all liquid metals. In Fig. 6 we report this product for many liquid metals calculated with the values of D, η_S, ρ, and T_m of Refs. 69–72. The values C_{Zw} scatter around the value for which $\eta_B/\eta_S\sim 0$, in fact, we obtain $D^{(R)}=0.0337$, $\eta_S^{(R)}=5.37$, and $C_{\text{Zw}}=0.181\pm 0.02$ as mean values that correspond for Eq. (10) to $\eta_B/\eta_S\simeq 0$. The values of D and η_S used in Fig. 6 are experimental values, smoothed by physical consideration of the models used and the scattering of the real experimental values is in some cases high, but not enough to affect the conclusion of this figure: if the Zwanzig relation is valid, the value of η_B is surely much lower than η_S, close to the m.p. for the liquid metals and particularly for the alkali metals, where the experimental error is lower. A way to check the validity of Eq. (10) is to use the data obtained from our simulation of liquid rubidium. In this case it is possible to calculate, in addition to self-diffusion and shear viscosity,

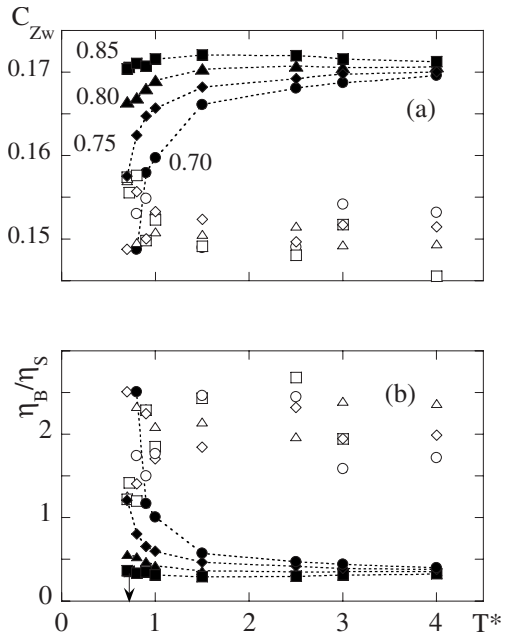

FIG. 8. (a) C_{Zw} of liquid argon as a function of temperature with the data of Ref. 75: results from the right (white symbols) and left (black symbols) sides of Eq. (10) are compared at $\rho^*=0.7,0.75,0.8,0.85$; (b) the black symbols are values of $\eta_B^*/\eta s^*$ calculated directly from the data of Ref. 75; the white symbols calculated from Eq. (10). The arrow on the abscissa of part (b) marks the value $T_m^*\sim 0.7$ of liquid argon ($\rho_m^*\sim 0.8$).

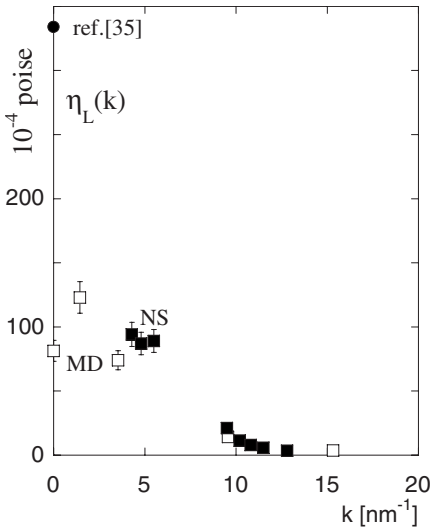

FIG. 9. $\eta_L(k)$ of liquid rubidium at $T=315$ K: the white (MD) and black (NS) squares are obtained from Eq. (1). The white square at $k=0$ is the MD value of η_L calculated via Green-Kubo relation, while the black circle at $k=0$ is the value obtained from the ultrasonic absorption measurements of Ref. 35. The figure also shows the estimated errors (note that, as reported in Ref. 35, the error on the ultrasound data may be greater than 50%).

also the right hand side of Eq. (10), by means of the derived values of longitudinal and bulk viscosities. The results are reported in Fig. 7 and it is apparent that the Zwanzig relation works well at the melting point while at higher temperatures it tends to overestimate the values of bulk viscosity.

In this figure, also the temperature dependence of C_{Zw} is shown for real liquid rubidium. C_{Zw}, as temperature increases, decreases slowly from the value at the m.p. reported in Fig. 6. The accuracy of Zwanzig's formula around the melting point is further supported by the results of Fig. 8. Here we show the results of a comprehensive study of transport properties of the Lennard-Jones fluid, in a wide range of thermodynamic states, from the triple point to low density gaseous states.[75] Using these data, the two values that result from the left and the right hand sides of Eq. (10) tend to converge at the melting point [see Fig. 8(a)]. Note that the melting point of liquid argon corresponds to $\rho_m^*\simeq 0.8$ and $T_m^*\simeq 0.7$ in reduced unit for a Lennard-Jones model. In that case, $C_{\mathrm{Zw}}\sim 0.155$ and, as a consequence, $\eta_B/\eta_S\sim 1.5$.

IV. CONCLUSIONS

By MD simulation, we have obtained a good agreement with neutron scattering results of $S(k)$ at $k\simeq k_{\max}$ (Sec. III A) in the whole temperature range. As this agreement extends to $\tilde{S}(k_{\max},\omega=0)$ and to the linewidths we can assume that the time dependence of the dynamic structure factor around the de Gennes narrowing zone is correctly accounted for. Moreover, also the longitudinal viscosity behavior is well reproduced, except for a small difference at the lowest temperature. Our MD simulation yields a generalized shear viscosity larger than the longitudinal and bulk viscosities at $k\simeq k_{\max}$. Shear and bulk viscosities, however, share a similar temperature dependence, with a decrease of $\sim 30\%$ as temperature increases. On the other hand, the longitudinal viscosity depends weakly on temperature $[(10\pm 15)\,\%]$. The good results mentioned above have suggested extending the comparison with experimental data of other dynamical properties. The self-diffusion coefficient (Sec. III B) also turns out to be in good accord with the measured values and the results deduced from the long time part of the intermediate MD scattering function $F_S(k_{\max},t)$ show a deviation from Fick's law in quantitative agreement with that observed for other alkali metals and predicted by mode coupling theory.

Calculated and experimental thermal conductivity values are very different, the MD value being lower than the experimental one by a factor of ~ 300 (Sec. III C), as expected due to the lack of the electronic contribution in our potential model. This may be corrected adopting an expanded model or *ab initio* molecular dynamics as shown in Refs. 12 and 38–40.

The other collective dynamical properties we focus on are the longitudinal, shear, and bulk viscosities, whose $k=0$ values are discussed in Sec. III D. There is a good agreement with the experiment for the shear viscosity and also for the temperature dependence of this quantity. On the contrary, the MD bulk viscosity, derived from the Green-Kubo relation, is much smaller than the experimental values obtained from ultrasound measurements.[35] This unexpected strong disagreement cannot be traced back to the missing electronic contribution, which is completely negligible in liquid metals, according to an ion-plasma-like approach.[52–54] The applica-

tion of the Zwanzig approach[66] to almost all liquid metals (see Fig. 6) supports our point of view that the large values of the bulk viscosity for the alkali metals may be a consequence of the large error in the calculation by Eq. (6) from the data of ultrasound measurements.

This large difference of bulk (and consequently longitudinal) viscosity is by no means a minor effect, as we demonstrate in Fig. 9, where we compare the k-dependent longitudinal viscosity, $\eta_L(k)$, from very recent NS results[14] to the corresponding MD values. Both sets of results have been obtained according to Eq. (1), at a temperature slightly above melting ($T=315$ K). The simulation data show a small maximum, due to a maximum in the k dependence of the bulk viscosity, and seem reasonably well connected with the Green-Kubo $k=0$ value. The NS results, on the other hand, are in good agreement with the simulation results up to the minimum k value accessible by NS ($k\sim 4$ nm^{-1}). An extension to smaller k values for the experimental data points would be desirable. Our MD and NS values near the structure factor maximum agree very well with results from Ref. 13. Included in the figure is a longitudinal viscosity value obtained from ultrasound absorption measurements,[35] which deviates distinctly from the MD result by about a factor of 3. We argue that the MD and NS k dependence of η_L suggests a much smaller longitudinal viscosity and hence also a much smaller bulk viscosity.

In conclusion, our suggestion is that the high value of the experimental bulk viscosity is an artifact produced by the large contribution to the error in its calculation from all of the quantities used in Eq. (6). In particular, the second term in parentheses is dominant for liquid metals, although practically negligible in nonmetallic liquids. As a consequence, in alkali metals, and probably in most liquid metals as well, bulk viscosity may be much lower than shear viscosity. From the computational point of view, we suggest to extend the *ab initio* simulation to bulk viscosity recently applied for the calculation of shear viscosity[64] in iron-sulfur and aluminum, in order to confirm the negligible contribution of the electrons to bulk and longitudinal viscosities.

*Author to whom correspondence should be addressed. davide@ipcf.cnr.it

[1] N. H. March, *Liquid Metals Concept and Theory*, Cambridge Monographs on Mathematical Physics (Cambridge University Press, Cambridge, 2005).
[2] U. Mizutani, *Introduction to Electron Theory of Metals* (Cambridge University Press, Cambridge, 2003).
[3] T. Scopigno, G. Ruocco, and F. Sette, Rev. Mod. Phys. **77**, 881 (2005).
[4] W.-C. Pilgrim and Chr. Morkel, J. Phys.: Condens. Matter **18**, R585 (2006).
[5] L. E. Gonzalez, D. J. Gonzalez, and J. M. Lopez, J. Phys.: Condens. Matter **13**, 7801 (2001).
[6] D. K. Belashchenko, High Temp. **44**, 675 (2006); W. Hu and F. Masahiro, Modell. Simul. Mater. Sci. Eng. **10**, 707 (2001); A. Avinc and V. I. Dimitrov, Comput. Mater. Sci. **13**, 211 (1999), and references therein.
[7] G. Kresse and J. Hafner, Phys. Rev. B **47**, 558 (1993); G. Kresse and J. Furthmüller, Comput. Mater. Sci. **6**, 15 (1996), and references therein.
[8] D. J. Gonzalez, L. E. Gonzalez, and M. J. Stott, Phys. Rev. B **74**, 014207 (2006), and references therein.
[9] R. Stadler, D. Alfè, G. Kresse, G. A. de Wijs, and M. J. Gillan, J. Non-Cryst. Solids **250-252**, 82 (1999).
[10] E. Burkel, J. Non-Cryst. Solids **250-252**, 70 (1999), and references therein.
[11] M. Ross, L. H. Yang, and W.-C. Pilgrim, Phys. Rev. B **74**, 212302 (2006).
[12] V. Recoules and J.-P. Crocombette, Phys. Rev. B **72**, 104202 (2005).
[13] F. Demmel, A. Diepold, H. Aschauer, and C. Morkel, Phys. Rev. B **73**, 104207 (2006).
[14] F. Demmel, D. Pasqualini, and C. Morkel, Phys. Rev. B **74**, 184207 (2006).
[15] D. L. Price, K. S. Singwi, and M. P. Tosi, Phys. Rev. B **2**, 2983 (1970); W.-M. Shyu, K. S. Sinwi, and M. P. Tosi, *ibid.* **3**, 237 (1971).
[16] U. Balucani, A. Torcini, and R. Vallauri, Phys. Rev. B **47**, 3011 (1993).
[17] J. F. Wax, R. Albaki, and J. L. Bretonnet, Phys. Rev. B **65**, 014301 (2001).
[18] D. Bertolini and A. Tani, J. Chem. Phys. **115**, 6285 (2001).
[19] J. R. D. Copley and J. M. Rowe, Phys. Rev. A **9**, 1656 (1974); E. G. D. Cohen, P. Westerhuijs, and I. M. de Schepper, Phys. Rev. Lett. **59**, 2872 (1987).
[20] W.-C. Pilgrim, R. Winter, F. Hensel, C. Morkel, and W. Gläser, Ber. Bunsenges. Phys. Chem. **95**, 1133 (1991); W.-C. Pilgrim, R. Winter, and F. Hensel, J. Phys.: Condens. Matter **5**, B183 (1993); R. Winter, W.-C. Pilgrim, and F. Hensel, *ibid.* **6**, A245 (1994); W.-C. Pilgrim, M. Ross, L. H. Yang, and F. Hensel, Phys. Rev. Lett. **78**, 3685 (1997).
[21] Chr. Morkel, T. Bodensteiner, and H. Gemperlein, Phys. Rev. E **47**, 2575 (1993).
[22] P. Chieux, J. Dupuy-Philon, J. F. Jal, and J. B. Suck, J. Non-Cryst. Solids **207-209**, 370 (1996).
[23] A. Rahman, Phys. Rev. A **9**, 1667 (1974).
[24] K.-E. Larsson and W. Gudowski, Phys. Rev. A **33**, 1968 (1986).
[25] U. Balucani, R. Vallauri, and T. Gaskell, Phys. Rev. A **35**, 4263 (1987); U. Balucani, A. Torcini, and R. Vallauri, *ibid.* **46**, 2159 (1992); D. Pasqualini, R. Vallauri, F. Demmel, Chr. Morkel, and U. Balucani, J. Non-Cryst. Solids **250-252**, 76 (1999).
[26] G. Kahl and S. Kambayashi, J. Phys.: Condens. Matter **6**, 10897 (1994); **6**, 10923 (1994).
[27] S. Munejiri, F. Shimojo, and K. Hoshino, J. Phys.: Condens. Matter **12**, 4313 (2000).
[28] A. Norden and A. Lodding, Z. Naturforsch. A **22A**, 215 (1967); these data fit very well with the empirical relationship $D=6.6\times 10^{-4}\exp(-8290/RT)$ reported in W. Ohse, *Handbook of Thermodynamic and Transport Properties of Alkali Metals* (Blackwell, Oxford, 1985).

[29] S. J. Larsson, C. Roxberg, and A. Lodding, Phys. Chem. Liq. **3**, 137 (1972): the continuous curve is the fit of the experimental data, $D=0.272\times(T/T_m)^{2.46}$, reported from the authors.
[30] J. L. Bretonnet, J. Chem. Phys. **120**, 11100 (2004).
[31] C. Fiolhais, J. P. Perdew, S. Q. Armster, J. M. MacLaren, and M. Brajczewska, Phys. Rev. B **51**, 14001 (1995); **53**, 13193 (1996).
[32] L. E. Gonzalez, D. J. Gonzalez, and J. Casas, J. Non-Cryst. Solids **312-314**, 158 (2002), and references therein.
[33] G. Marechal and J. P. Ryckaert, Chem. Phys. Lett. **101**, 548 (1983).
[34] D. Bertolini and A. Tani, Phys. Rev. E **56**, 4135 (1997); U. Balucani, D. Bertolini, A. Tani, and R. Vallauri, J. Chem. Phys. **112**, 9025 (2000).
[35] M. G. Kim, K. A. Kemp, and S. V. Letcher, J. Acoust. Soc. Am. **49**, 706 (1971), and references therein.
[36] J. M. Ziman, *Electrons and Phonons* (Clarendon, Oxford, 1960).
[37] E. Yamasue, M. Susa, H. Fukuyama, and K. Nagata, Int. J. Thermophys. **24**, 713 (2003); M. V. Peralta-Martinez and W. A. Wakeham, *ibid.* **22**, 395 (2001); B. Giordanengo, N. Benazzi, J. Vinckel, J. G. Gasser, and L. Roubi, J. Non-Cryst. Solids **250-252**, 377 (1999).
[38] R. Redmer, H. Reinholz, G. Röpke, R. Winter, F. Noll, and F. Hensel, J. Phys.: Condens. Matter **4**, 1659 (1992).
[39] P. L. Silvestrelli, A. Alavi, and M. Parrinello, Phys. Rev. B **55**, 15515 (1997).
[40] F. Shimojo, Y. Zempo, K. Hoshino, and M. Watabe, J. Non-Cryst. Solids **205-207**, 893 (1996).
[41] W. D. Weatheford, R. K. Johnston, and M. L. Valtierra, J. Chem. Eng. Data **9**, 520 (1964).
[42] E. E. Shpil'rain *et al.*, in *Handbook of Thermodynamic and Transport Properties of Alkali Metals*, edited by R. W. Ohse (Blackwell, Oxford, 1985).
[43] *Handbook of Thermodynamic and Transport Properties of Alkali Metals*, edited by W. Ohse (Blackwell, Oxford, 1985).
[44] O. J. Kleppa, J. Chem. Phys. **18**, 1331 (1950).
[45] J. K. Fink and L. Leibowitz, Report No. ANL/RE-95/2, 1995 (unpublished).
[46] S. V. Letcher and R. T. Beyer, J. Acoust. Soc. Am. **35**, 1571 (1963).
[47] J. M. Flinn, J. Jarzynski, and T. A. Litovitz, J. Chem. Phys. **54**, 4331 (1971).
[48] F. Eggers and U. Kaatze, Meas. Sci. Technol. **7**, 1 (1996); M. Musso, F. Aliotta, C. Vasi, R. Aschauer, A. Asenbaum, and E. Wilhelm, J. Mol. Liq. **110**, 33 (2004), and references therein.
[49] R. E. Graves and B. M. Argrow, J. Thermophys. Heat Transfer **3**, 337 (1999), and references therein.
[50] L. M. Berezhkovsky, A. N. Drozdov, V. Yu. Zitserman, A. N. Lagar'kov, and S. A. Triger, J. Phys. F: Met. Phys. **14**, 2315 (1984).
[51] Y. Zhang, G. Guo, and G. Nie, Phys. Chem. Miner. **27**, 164 (2000).
[52] P. Vieillefosse and J. P. Hansen, Phys. Rev. A **12**, 1106 (1975); B. Bernu and P. Vieillefosse, *ibid.* **18**, 2345 (1978).
[53] D. K. Chaturvedi and J. S. Thakur, Phys. Lett. **101A**, 408 (1984).
[54] M. P. Tosi, Nuovo Cimento Soc. Ital. Fis., D **14D**, 559 (1992).
[55] A. J. Zuckerwar and R. L. Ash, Phys. Fluids **18**, 047101 (2006); A. J. Zuckerwar, J. Acoust. Soc. Am. **105**, 2210 (1999).
[56] J. H. Lienhard IV and J. H. Lienhard V, *A Heat Transfer Textbook* (Philogiston, Cambridge, MA, 2004), p. 299.
[57] P. Gray and S. A. Rice, J. Chem. Phys. **41**, 3689 (1964).
[58] K. Rah and B. C. Eu, Phys. Rev. Lett. **83**, 4566 (1999); Phys. Rev. E **60**, 4105 (1999); J. Chem. Phys. **112**, 7118 (2000); **114**, 10436 (2001).
[59] H. Okumura and F. Yonezawa, Phys. Rev. E **67**, 021205 (2003); Physica A **321**, 207 (2003).
[60] J. Chihara and G. Kahl, Phys. Rev. B **58**, 5314 (1998).
[61] S. Munejiri, F. Shimojo, K. Hoshino, and M. Watabe, J. Non-Cryst. Solids **205-207**, 278 (1996).
[62] G.-X. Qian, M. Weinert, G. W. Fernando, and J. W. Davenport, Phys. Rev. Lett. **64**, 1146 (1990).
[63] F. Shimojo, Y. Zempo, K. Hoshino, and M. Watabe, Phys. Rev. B **52**, 9320 (1995).
[64] D. Alfè and M. J. Gillan, Phys. Rev. Lett. **81**, 5161 (1998); R. Stadler, D. Alfè, G. Kresse, G. A. de Wijs, and M. J. Gillan, J. Non-Cryst. Solids **250-252**, 82 (1999).
[65] J. Bosse, W. Götze, and M. Lücke, Phys. Rev. A **17**, 434 (1978).
[66] R. Zwanzig, J. Chem. Phys. **79**, 4507 (1983).
[67] N. H. March and M. P. Tosi, Phys. Rev. E **60**, 2402 (1999).
[68] D. M. Heyes and N. H. March, Int. J. Thermophys. **20**, 267 (1999).
[69] P. Protopapas, H. C. Andersen, and N. A. D. Parlee, J. Chem. Phys. **59**, 15 (1973).
[70] I. Yokoyama, Physica B **341**, 145 (2000); **269**, 244 (1999); **254**, 172 (1998).
[71] A. S. Chauhan, R. Ravi, and R. P. Chhabra, Chem. Phys. **252**, 227 (2000); S. G. Prakash, R. Ravi, and R. P. Chhabra, *ibid.* **302**, 149 (2004).
[72] V. G. Postovalov, E. P. Romanov, V. P. Kondrat'ev, and V. I. Kononenko, High Temp. **41**, 762 (2003).
[73] M. Dzugutov, Nature (London) **381**, 137 (1996).
[74] Y. Rosenfeld, J. Phys.: Condens. Matter **11**, 5415 (1999), and references therein.
[75] K. Meier, *Computer Simulation and Interpretation of the Transport Coefficients of the Lennard-Jones Model Fluid* (Shaker, Aachen, 2002); K. Meier, A. Laesecke, and S. Kabelac, J. Chem. Phys. **122**, 014513 (2005); **121**, 3671 (2004); **121**, 9526 (2004).